Fields and Filaments in the Core of the Centaurus Cluster

G. B. Taylor[1], A. C. Fabian[2], G. Gentile[1], S. W. Allen[3], C. Crawford[2] and J. S. Sanders[2]

1. University of New Mexico, Dept. of Physics and Astronomy, Albuquerque, NM 87131, USA; gbtaylor@unm.edu
2. Institute of Astronomy, Madingley Road, Cambridge CB3 0HA, acf@ast.cam.ac.uk; csc@ast.cam.ac.uk
3. Kavli Institute of Particle Astrophysics and Cosmology, Stanford University, Stanford, CA 94305, USA; swa@stanford.edu

24 August 2007

ABSTRACT

We present high resolution images of the Faraday Rotation Measure (RM) structure of the radio galaxy PKS 1246−410 at the center of the Centaurus cluster. Comparison with Hα-line and soft X-ray emission reveals a correspondence between the line-emitting gas, the soft X-ray emitting gas, regions with an excess in the RM images, and signs of depolarization. Magnetic field strengths of 25 μG, organized on scales of ∼1 kpc, and intermixed with gas at a temperature of 5×10^6 K with a density of ∼0.1 cm^{-3} can reproduce the observed RM excess, the depolarization, and the observed X-ray surface brightness. This hot gas may be in pressure equilibrium with the optical line-emitting gas, but the magnetic field strength of 25 μG associated with the hot gas provides only 10% of the thermal pressure and is therefore insufficient to account for the stability of the line-emitting filaments.

Key words: galaxies: magnetic fields – galaxies: active – galaxies: nuclei – galaxies individual: PKS 1246−410– radio continuum: galaxies – X-rays: galaxies: clusters

1 INTRODUCTION

The Centaurus cluster, Abell 3526, is a nearby (redshift z=0.0104), X-ray bright galaxy cluster. At the center of this cluster is the bright elliptical galaxy NGC 4696, hosting the moderately powerful radio source, PKS 1246−410. We have been engaged in detailed studies of the X-ray and radio emission from this cluster (Sanders & Fabian 2002, Taylor, Fabian & Allen 2002), and have recently obtained a further 200 ksec of Chandra data (Fabian et al. 2005). The new Chandra image reveals a complex structure within the central few kiloparsecs. A plume-like structure swirls clockwise to the NE and wraps around the radio source. There are clear signs of interaction between the X-ray and radio emission including: (1) strong X-ray emission that matches the shape of the radio emission just south of the core; (2) a faint rim of hard X-ray emission along the northern edge of the radio source; and (3) deep cavities in the X-ray emission on both the east and west sides. We also find a compact X-ray component coincident with the radio and optical core (Taylor et al. 2006).

From VLA data primarily in BnA configuration, Taylor et al. (2002) imaged the rotation measure (RM) distribution across PKS 1246−410 at a resolution of 2.1 × 1.2 arcsecond. The RMs appear patchy and are typically in the range −500 to +500 rad m^{-2}, with a maximum absolute value of ∼1800

rad m^{-2}. Assuming that the RMs are produced by cluster magnetic fields as found for other galaxies at the center of dense clusters (see review by Carilli & Taylor 2002), simple magnetic field topologies lead to estimates of the magnetic field strength of ∼11 μG. The Centaurus cluster is exceptional in that the radio source PKS 1246−410 provides a well resolved probe of the central 10 kpc of a cooling core cluster.

Taylor et al. (2002) suggested that some regions of higher RM lay behind regions of high X-ray surface brightness. This raised the possibility that (1) some of the bright inner X-ray emission is located in front of the radio source; and (2) this thermal gas within a few kiloparsecs of the radio could contribute significantly to the RM. Rudnick & Blundell (2003) used the observations of Taylor et al. to investigate the possibility of a local cocoon producing the high RMs, and claimed to find evidence for this in a correlation between the intrinsic polarization angles and the RM. However, Ensslin et al. (2003) showed that the relationship was an artifact of the analysis used, and a better formed statistic showed no correlation. Here, we present improved observations of the RM structure in PKS 1246−410 and further explore the evidence for local interactions through detailed comparison with X-ray and Hα images.

The arc-shaped structures seen in the Hα filaments appear quite smooth with no indication on subkiloparsec
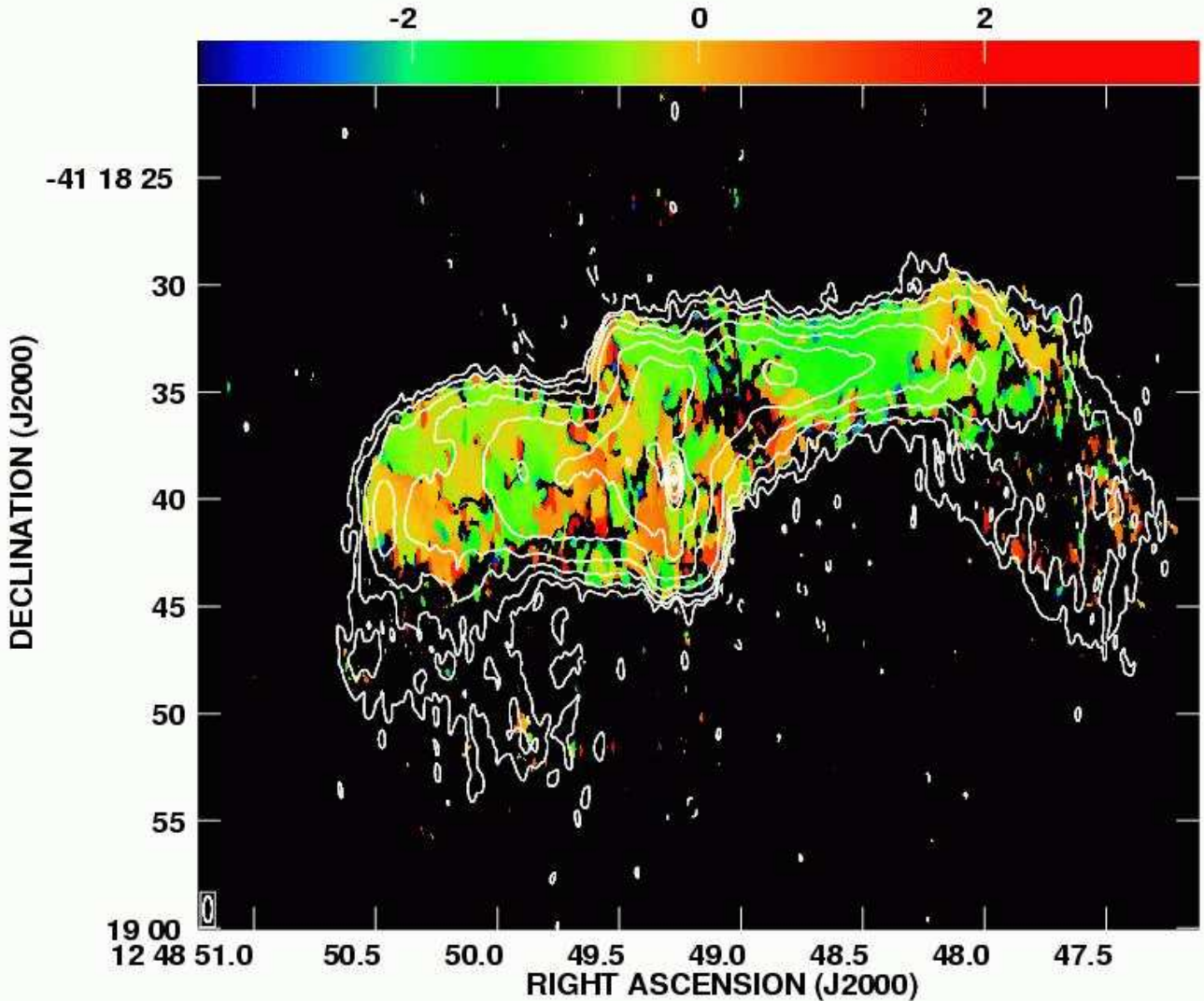
Figure 1. The rotation measure (RM) map for PKS 1246−410 with contours from the 5 GHz total intensity image overlaid. Contours start at 0.15 mJy/beam and increase by factors of 2. The angular resolution is 1.2×0.4 arcsec.

scales of surrounding turbulence (Crawford et al. 2005). This smoothness, and the commonality of structure between optical filaments, X-ray arcs, and the dust lanes suggest that these could all have been shaped by strong magnetic fields. An alternative explanation could be a bulk laminar flow within the intracluster medium. Detailed comparisons between the Faraday rotation measure and the optical filaments should allow us to measure the strength of the magnetic fields in the region of the filaments and thereby discriminate between these two possibilities.

Here we present VLA (Very Large Array)[1] observations of the radio galaxy PKS 1246−410 at the centre of the Centaurus cluster. In §2 we describe the radio observations. In §3 we summarize the Hα emission, and in §4 we summarize the X-ray observations. In §5 we discuss the radio properties

of PKS 1246−410 and in §6 we compare the multi-wavelength observations and consider the origin of the observed RMs.

We assume $H_0 = 71$ km s^{-1} Mpc^{-1} and $\Omega = 1$ so that $1'' = 210$ pc at the redshift (0.0104) of the Centaurus cluster.

2 RADIO OBSERVATIONS AND DATA REDUCTION

Observations of PKS 1246−410 were made at 4.635, 4.885, 8.115, and 8.485 GHz at the VLA in its A configuration on 2006 February 8. The source 3C 286 was used as the primary flux density calibrator, and as an absolute reference for the electric vector polarization angle (EVPA). Phase calibration was derived from the nearby compact source J1316−3338 with a cycle time between calibrators of about 16 minutes. Instrumental calibration of the polarization leakage terms was obtained using OQ 208 which was observed over a wide range in parallactic angle. The data were reduced in AIPS (Astronomical Image Processing System), following

---
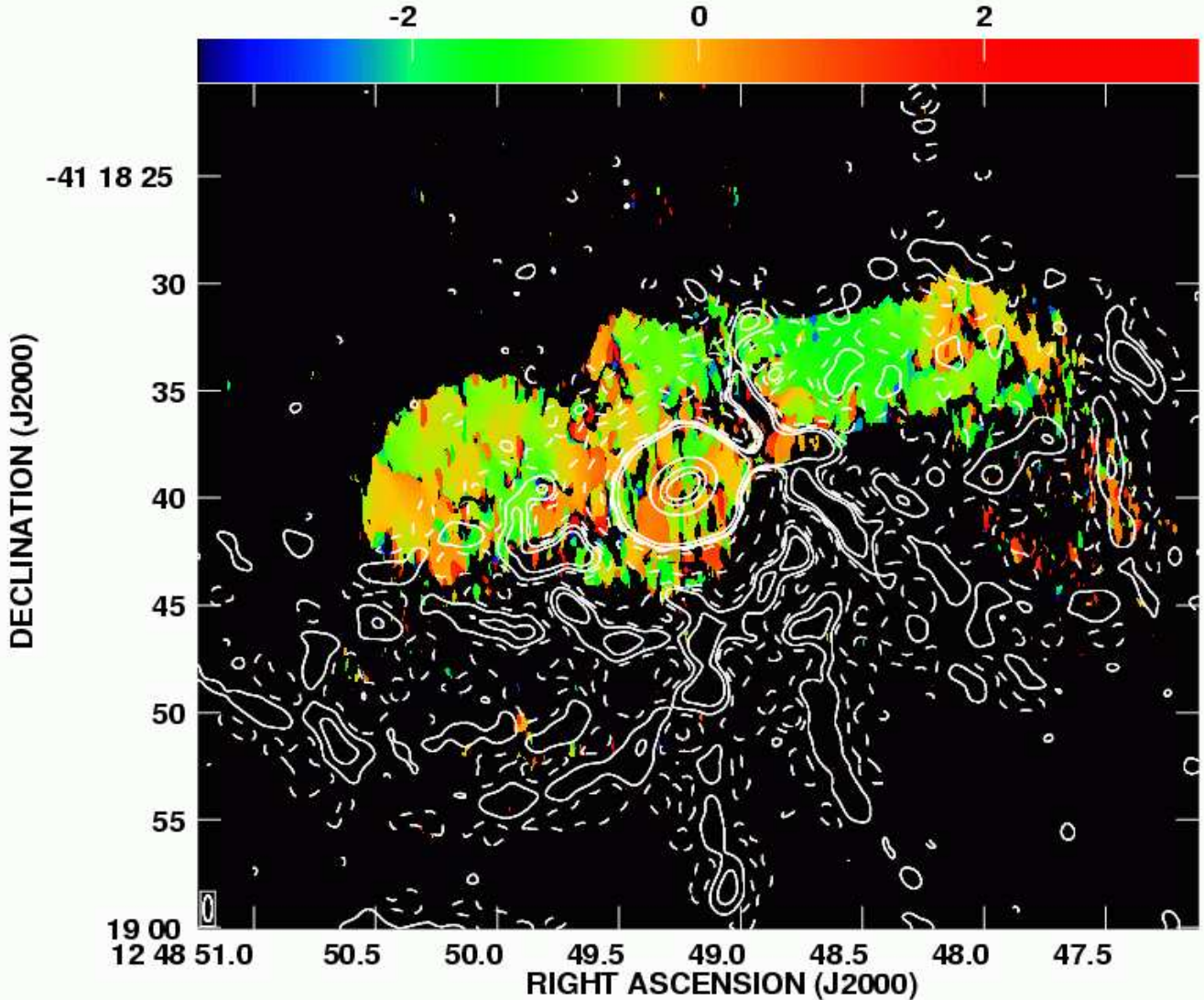
Figure 2. The rotation measure (RM) map for PKS 1246‒410 with contours from the unsharp-masked Hα image overlaid. The color bar ranges from −3500 to 3500 rad m⁻². Relative contours are drawn starting at 2.5σ and increasing by factors of 4 (Crawford et al. 2005).

the standard procedures. The AIPS task IMAGR was used with a suitable taper to make Stokes I, Q and U images at each of the 4 frequencies observed at the same resolution. Polarized intensity, P, images and polarization angle, χ, images were derived from the Q and U images. The Faraday Rotation Measure (RM) image was made from the combination of the χ images. Pixels in the RM image were flagged when the error in any of the χ images exceeded 20 degrees.

3   Hα OBSERVATIONS

A detailed study of the extended Hα filaments surrounding PKS 1246‒410 has recently been published by Crawford et al. (2005). They find a network of line-emitting filaments extending over the central 50 arcsec (10.5 kpc). These filaments correlate with arc-like plumes seen in soft X-ray emission. Crawford et al. speculate that both the Hα filaments

and the plumes of soft X-ray emitting gas have been drawn out of the center by buoyant bubbles created by the central radio galaxy, PKS 1246‒410.

4   X-RAY OBSERVATIONS

Fabian et al. (2005) presented deep (199 ksec) observations of the Centaurus cluster, that showed well defined cavities coincident with PKS 1246‒410. Further evidence of outbursts from the radio galaxy were seen in semi-circular edges to the east and west marked by sharp temperature increases.

The electron density derived at the inner 70 kpc (4.2′) radius region, determined from a deprojection analysis, is shown in Taylor et al. (2002). The best-fitting $\beta-$model for the density has parameter values $n_0 = 0.099 \pm 0.001$ cm⁻³, $\beta = 0.39\pm0.01$, and a core radius, $r_c = 5.4\pm0.3$ kpc. Sanders & Fabian (2006) find a central temperature of $\sim 2 \times 10^7$ K

in the lobes. Note that the core size is similar to that of the radio source, which has made 'holes' in the X-ray emission at radii of 1–5 kpc.

5 RADIO PROPERTIES OF PKS 1246−410

The radio source PKS 1246−410 is associated with NGC 4696, an elliptical galaxy at the center of the Centaurus cluster (also known as Abell 3526). The radio power of PKS 1246−410 is 1.5×10^{24} W Hz^{-1} at 1.6 GHz, identifying it as a low power radio galaxy for which we would expect an FR I morphology (edge dimmed extended radio tails). In fact the radio morphology at 5 GHz, shown in Fig. 1, appears quite different from most low power radio galaxies (Parma et al. 1987). The usual well defined core and thin jets feeding into larger lobes are missing. Instead there is a bright point source which we identify as the core based on its central location and slightly flatter spectral index, $\alpha = -0.5$ where $S_\nu \propto \nu^\alpha$ (Taylor et al. 2002). The properties of the core were further examined by Taylor et al. (2006) who found it to be radiatively underluminous but powering a jet (detected by the VLBA) that carries off enough energy to inflate the cavities seen in the thermal gas.

The bright radio lobes of PKS 1246−410 are moderately well polarized ($4 - 40\%$), so it is possible to derive the RM distribution across nearly the entire radio source. This was done by Taylor et al. (2002) at a resolution of 2.1×1.2 arcseconds. The RMs appear patchy and are not correlated with any features in total intensity.

We combine our new VLA-A configuration observations at 5 and 8.4 GHz with the previous observations. Our higher angular resolution (1.2×0.4 arcsec) images reveal some fine-scale structure in the Faraday rotation measure image (Fig. 1). In general the western lobe appears to have smoother RMs with typical values of -1000 rad m^{-2} over a $5''$ region. Much of the eastern lobe is patchy with a scale size of $\sim 2''$ (0.4 kpc). Typical RM gradients are ~ 400 rad m^{-2}/arcsec. Exceptionally large RM gradients are found in the regions spatially coincident with Hα filaments. These regions are up to 2 arcseconds (0.4 kpc) wide and 5 arcsec (1 kpc) long.

Very little polarization is detected after the radio lobes bend toward the south, but this is most likely due to a lack of sensitivity since the lobes fade at 8.4 GHz to 100-300 μJy/beam and below. Given our noise level of ~ 25 μJy we would only detect polarization (at the 2 σ level) if it was as high as 20-50%. There is a hint of an anti-correlation with line emission across the southwest lobe, but more sensitive observations will be required to confirm low fractional polarization there.

6 CONTRIBUTORS TO THE FARADAY ROTATION

We can rule out uniform internal Faraday rotation since it deviates from a wavelength-squared law for changes in angle of more than 90 degrees (Burn 1966). Internal Faraday rotation also predicts significant depolarization of the radio source since emission produced at the back interferes with emission produced at the front. The RM of 2000 rad m^{-2}
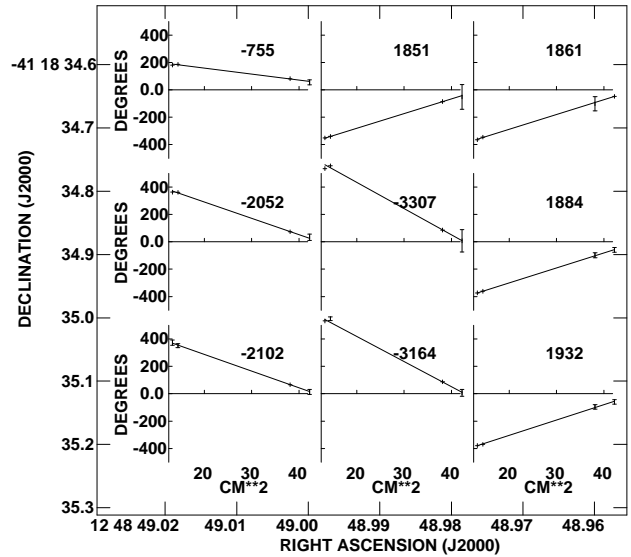
Figure 3. Fits to the electric vector position angle as a function of wavelength squared in the western filament. The slope of the fit provides the RM and is indicated for each pixel. The transition from -2000 rad m^{-2} to $+2000$ rad m^{-2} occurs over just $0.6''$.

seen in PKS 1246−410 corresponds to a change in angle of 400 degrees at 5 GHz.

Faraday rotation from an external screen is thus likely and could have contributions from (1) optical line-emitting filaments crossing in front of the radio lobes; (2) the filaments of dense soft X-ray emitting gas on 10-kpc scales; (3) a mixing layer between source fields and the surrounding medium (Rudnick & Blundell 2003); and (4) the 100-kpc scale cluster gas (Taylor et al. 2002). The latter two explanations do not readily explain fine scale RM structures correlated with the Hα filaments so we do not consider them further here.

For external Faraday rotation, the RMs are related to the density, n_e, and magnetic field along the line-of-sight, $B_\parallel$, through the cluster (or line-emitting gas) according to

$$RM = 812 \int_0^L n_e B_\parallel \, \mathrm{d}l \ \text{radians m}^{-2} \, , \qquad (1)$$

where $B_\parallel$ is measured in μGauss, n_e in cm^{-3} and dl in kpc.

6.1 Hα/Radio Comparisons

Depolarization of the radio source coincident with the line-emitting gas has been seen before (e.g., A1795; Ge & Owen 1993), and claimed to be the result of large RM gradients within the synthesised beam. Even modest magnetic field strengths, combined with the high thermal densities of the line-emitting gas, can produce large RM gradients. In Fig. 2 we show overlays of the unsharp-masked Hα and the RM map. Inspection of Fig. 2 reveals that RM image has values near the extreme ranges of the image and fewer measurements (presumably due to depolarization of the radio
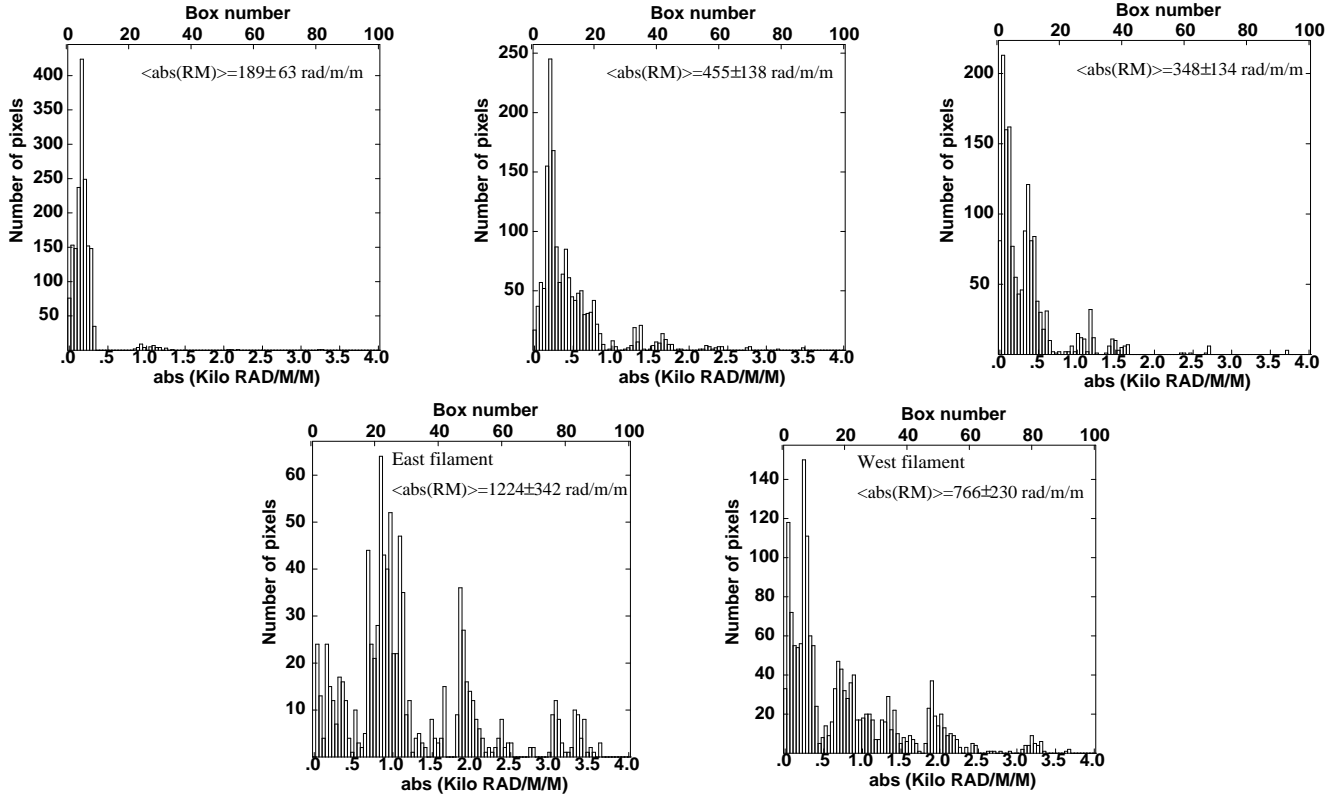
Figure 4. Absolute rotation measure distributions for selected areas in PKS 1246−410. The top three regions were selected by taking a random starting position in the east lobe and then spacing over at regular intervals of 8.8 arcseconds. The bottom two regions correspond to the eastern and western filaments. The width of each bin is 40 rad m^{-2}, which is about the same as the error in the RM determination for any given point. The number of independent beams is: 11.1, 10.5, and 9.9 respectively for the 3 regions plotted on the top row; and 6.1 and 10.7 for the east and west filament, respectively.

source) where the Hα filaments cross the lobes. We find values ranging from −2000 rad m^{-2} to +2000 rad m^{-2} on scales of ∼ 0.4″(the maximum resolution of our observations). These correspond to gradients of 10^4 rad m^{-2}/arcsec.

A concern about the measurements of the RMs in the filaments is that they are in regions of relatively low SNR. To make sure that the high RMs are not due to low SNR, we show the RM fits in the west filament in Fig. 3. The EV-PAs are well fit by a λ^2-law, and have reasonable reduced χ^2 values of ∼1, with a few fits as low as 0.1 and as high as 10. To further test the possibility that the RMs are higher in association with the filaments we compare the absolute RM distribution in three regularly spaced regions with a similar area, with those just coincident with the filaments (Fig. 4). The average |RM| in the east and west filaments is 1224 ± 342 rad m^{-2} and 766 ± 230 rad m^{-2}, compared to averages of below 500 rad m^{-2} for the three typical regions. We performed a Kolmogorov-Smirnov test (KS-test) to see how significant the difference is, and found that the three typical regions have a > 99.9% probability of being drawn from a different population compared to the filament regions. We also checked for any correlation between low SNR and high RM. In general regions of low SNR are equally likely to have any RM, and are not biased to large absolute values. We conclude that there is a real association between the Hα emission and the regions of enhanced RM.

The surface brightness of the filaments in Hα+[NII] is

1-3 × 10^{-16} erg cm^{-2} s^{-1} arcsec^{-2} (Crawford et al. 2005). If we take 2 × 10^{-16} erg cm^{-2} s^{-1} arcsec^{-2} for Hα in the brightest depolarizing part, 5 arcsec (∼1 kpc) west of the nucleus, and adopt a product $nT = 2 × 10^6$ cm^{-3} K for the surrounding gas pressure (taking values from Allen et al. 2006), we find that the depth of the Hα emitting region (T ∼ 10^{4}K) is 0.01 pc. This assumes a uniform covering fraction. The line-emitting gas is much more likely to be in the form of a network of small filaments, in which case the covering fraction is smaller and the depth proportionately larger, realistically ∼1 pc. If the magnetic fields are organized on similar scales then the many field reversals within the synthesized beam (dimensions 252 × 84 parsec), would scramble the intrinsic polarization vectors, and lead to depolarization. Even if the magnetic fields are for some reason organized on kiloparsec scales such a network of filaments could not provide the observed high RM values as they would still produce larger RM gradients than we observe and would completely depolarize the radio emission due to variations within the synthesized beam. Therefore, even though the Hα emission is coincident with regions of enhanced RM, it does not have the proper physical characteristics to produce coherent RMs on the observed scales.
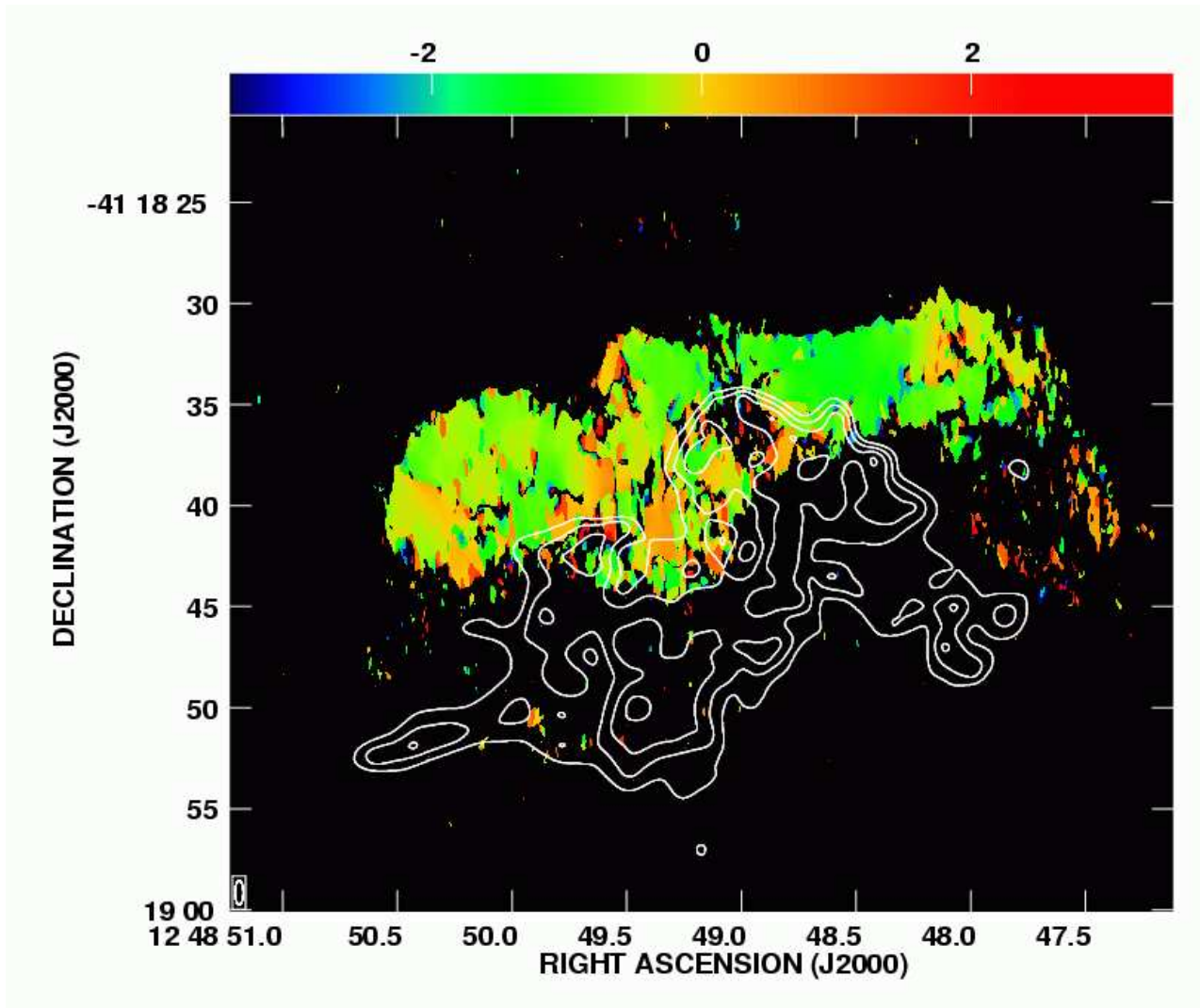
Figure 5. Overlay of the Faraday RM on the X-ray temperature map. The innermost (highest) contours correspond to temperatures of 0.5 keV and the lowest contours to 0.9 keV. The temperatures over most of the upper part of the radio lobes are around 1.5 keV.

6.2 Soft X-ray/Radio Comparisons

As pointed out by Crawford et al. (2005) the soft X-ray emitting gas is coincident with the optical line filaments. In Fig. 5 we overlay the X-ray temperature map from Crawford et al. on our Faraday RM image. A clear correspondence can be seen between low temperature gas and the regions of the east and west filaments previously noted to have large RM gradients.

A contribution to the RM could come from the dense soft X-ray emitting gas, of density 0.1 cm^{-3} (Allen et al 2006). This gas has a covering fraction closer to unity and is much more volume filling than the line emitting gas outside the radio bubble. Then, if its depth is about 1 kpc, the magnetic field required to produce the RMs observed of $\sim$2000 rad m^{-2} is about 25 μG. The magnetic pressure is then 2×10^5 cm^{-3} K, or about 10 per cent of the thermal pressure. These values seem reasonable and given the good correspondence with the soft X-ray emitting gas we believe this is the most likely cause for the excess RMs and RM gradients observed.

A simple model where tangled magnetic flux is conserved as gas cools at constant pressure would predict that $B \propto T^{-2/3}$. This is in rough agreement with the increase in B from ~ 11 to 25μG expected as the temperature drops from 1.5 to ~ 0.6 keV. If this scaling continues to lower temperature the gas at ~ 0.1 keV (10^6 K) would have a magnetic pressure similar to the thermal pressure. The optical filaments may well have significant magnetic pressure, likely needed for maintaining their integrity against shredding by random motions and conduction. Our observations are however unable to comment directly on them due to their very small scale (section 6.1).

7 CONCLUSIONS

New VLA observations of the radio galaxy PKS 1246-410, providing high angular and spatial resolution, afford us with a rare case where we can sample the RM structure continuously across the core of a cluster. We find distinct regions, of width $\sim$400 pc, where the RM and RM gradients, are

Table 1. Observational Parameters

Source	Date	Frequency (GHz)	Bandwidth[a] (MHz)	Config.	Duration (hours)
PKS 1246	Apr1998	1465/1565	25	A	0.24
-410	Jun1998	1465/1565	25	BnA	0.99
	Apr1998	4635/4885	50	A	0.09
	Jun1998	4635/4885	50	BnA	1.23
	Nov1998	4635/4885	50	CnB	0.61
	Jun1998	8115/8485	50	BnA	0.89
	Nov1998	8115/8485	50	CnB	0.62

enhanced, and the fractional polarization is reduced. This enhancement in the RM most likely originates in dense, soft X-ray emitting gas in front of the radio lobe. The magnetic fields required to produce the observed enhancement are 25 μG, similar to the equipartition estimates for the magnetic fields interior to the lobes, and a few times larger than the ambient cluster magnetic fields. If the magnetic fields continues to increase as the gas cools according to $B \propto T^{-2/3}$ then the fields may play an important role in shaping the optical filaments. To confirm this scenario would require observations with at least an order of magnitude higher angular resolution, and a hundredfold increase in sensitivity, such as could be provided by the proposed Square Kilometer Array. Observations of the RM structure in other clusters can be obtained now with the VLA and some effort, and will soon be made much easier by the advent of the EVLA. These radio observations can be compared to sensitive X-ray images to look for similar correlations between RM enhancements and soft X-ray emission.

REFERENCES

Allen, S.W., Fabian, A.C., Johnstone, R.M., Arnaud, K.A., Nulsen, P.E.J. 2001, MNRAS, 322, 589

Allen, S. W., Dunn, R. J. H., Fabian, A. C., Taylor, G. B., & Reynolds, C. S. 2006, MNRAS, 372, 21

Burn, B.F. 1966, MNRAS, 133, 67

Carilli, C.L., & Taylor, G.B. 2002, ARA&A, 40, 319

Crawford, C. S., Hatch, N. A., Fabian, A. C., & Sanders, J. S. 2005, MNRAS, 363, 216

Ensslin, T. A., Vogt, C., Clarke, T. E., & Taylor, G. B. 2003, ApJ, 597, 870

Fabian, A. C., Sanders, J. S., Taylor, G. B., & Allen, S. W. 2005, MNRAS, 360, L20

Ge, J.-P., Owen, F.N. 1993, AJ, 105, 778

Ikebe Y., Makishima K., Fukazawa Y., Tamura T., Xu H., Ohashi T., Matsushita K., 1999, ApJ, 525, 58

Parma, P., de Ruiter, H. R., Fanti, C., Fanti, R., & Morganti, R. 1987, A&A, 181, 244

Rudnick, L., & Blundell, K. M. 2003, ApJ, 588, 143

Sanders, J.S., & Fabian, A.C. 2002, MNRAS, 331, 273

Sanders, J. S., & Fabian, A. C. 2006, MNRAS, 371, 1483

Taylor, G. B., Fabian, A. C., & Allen, S. W. 2002, MNRAS, 334, 769

Taylor, G. B., Sanders, J. S., Fabian, A. C., & Allen, S. W. 2006, MNRAS, 365, 705